대한체질인류학회지 제23권 제4호
Korean J Phys Anthropol Vol. 23, No. 4 (2010) pp. 187~198
Korean Journal of Physical Anthropology

Improved Sectioned Images of the Female Pelvis Showing Detailed Urogenital and Neighboring Structures

Sung Bae Hwang, Min Suk Chung[1], Yoon Ik Hwang[1], Hyo Seok Park[2], Dong-Hwan Har[3], Dong Sun Shin[1], Byeong-Seok Shin[4], Jin Seo Park[2]

Department of Physical Therapy, Kyungbuk College
[1]*Department of Anatomy, Ajou University School of Medicine*
[2]*Department of Anatomy, Dongguk University College of Medicine*
[3]*Graduate School of Advanced Imaging Science, Multimedia and Film, Chungang University*
[4]*Department of Computer Science and Information Engineering, Inha University*

(Received 8 December 2010, revised 18 December 2010, accepted 21 December, 2010)

Abstract : The sectioned images (SIs) of the pelvis from a female cadaver are the best source of realistic three-dimensional (3D) models of the female urogenital system. The purpose of this research is to present SIs and outlined images of the female pelvis with improved quality, which may be used to produce 3D models to simulate virtual dissection or surgery of the female urogenital and adjacent structures.

A pelvis of Korean female cadaver which preserved buttock curve was scanned with 3T MR and CT machines. The pelvis was embedded and milled at 0.1 mm intervals. All sectioned surfaces were photographed to create horizontal SIs. On the Photoshop, 73 structures were outlined in the SIs to create outlined images. Once the structures were outlined, volume and surface models of the structures could be produced.

A total of 222 MRIs and 222 CTs of a female pelvis were obtained. 2,220 SIs of the pelvis were obtained ($0.1 \times 0.1 \times 0.1$ mm^3-sized voxels; 48 bits color). 222 outlined images of 73 structures were prepared at 1 mm intervals. Once the structures were outlined, 3D volume and surface models of the structures were produced without the help of the computer programmers using MRIcro and Maya software.

We have produced high quality SIs of the female pelvis accompanied by corresponding MRI and CT images. 3D volume and surface models of the female pelvic structures have been constructed. These computerized models may serve as the basis for future realistic medical simulation programs that may enhance clinical understanding of pelvic anatomy.

Keywords : Cross-sectional anatomy, Magnetic resonance imaging, X-ray computed tomography, Three-dimensional imaging, Pelvis, Urogenital system

Introduction

The sectioned images (SIs) of the pelvis from a female cadaver enable the creation of realistic three-dimensional (3D) images and various educational tools of female urogenital system (Schiemann et al. 2000, Park et al. 2006, Pommert et al. 2006, Spitzer and Scherzinger 2006, Uhl et al. 2006). Up to this time, users have been able to utilize the SIs of female pelvis from the U.S. Visible Human Project (Ackerman 1999), the Stanford Visible Female (Heinrichs et al. 1996), the Chinese Visible Human (Zhang et al. 2006), and the Virtual Chinese Human (Yuan et al. 2008). However, the previous SIs have some limitations. In the Visible Human Project, the subject was post-menopausal, so the female genital organs, such as the uterus

*This research was supported by Basic Science Research Program through the National Research Foundation of Korea (NRF) (grant number 2010-0009950).
Correspondence to : Jin Seo Park (Department of Anatomy, Dongguk University College of Medicine)
E-mail : park93@dongguk.ac.kr

(A) (B) (C)

Fig. 1. (A) Horizontal and vertical lines on the cadaver's skin along the laser lights; (B) pelvis and abdomen blocks properly located in the embedding box, where embedding agent is poured; (C) photography of the sectioned surface using a digital camera.

and ovaries, are degenerated in the SIs. That is why the Stanford Visible Female was devised with a young female cadaver; but its SIs do not satisfy users in quality. In the Visible Human Project and Chinese Visible Human, the whole cadavers were laid on their backs so that buttocks contour was flat, which does not produce a good appearance of 3D images. The previous SIs involved both intervals and pixel size, which were 0.33 mm (Visible Human Project) or 0.2 mm (Chinese Visible Human, Virtual Chinese Human). The intervals and pixels are required to be smaller for identification of the fine structures. For making 3D images, users need not only SIs but also outlined images based on the SIs. The outlined images are neither sufficient nor readily obtainable from the former projects.

The objective of this study is to present SIs and outlined images of the female pelvis with improved qualities, which promote the two-dimensional or 3D atlases of the female urogenital system for learning topographic anatomy as well as the virtual reality simulators contributing to clinical practice in gynecology and urology. To achieve the objective, we tried to arrange a suitable female cadaver and improved instruments and techniques, which have been prepared for the Visible Korean, our project (Park et al. 2005b).

Materials and Methods

The donated cadaver of a 43-year-old Korean female, 1,520 mm in height and weighing 54 kg, was selected. She died of suicide by hanging and had suffered from alcoholism, and her body was donated for medical research according to the agreement by her family. We found no external injuries involving the pelvis. The cadaver was placed in the prone position and the flattened buttocks were massaged to revive the natural contour of the gluteal region. No fixatives or dyes that would alter the tissue colors were injected.

During MR scanning, the horizontal plane of the cadaver pelvis was identified. The cadaver in the prone position was placed on the bed of a MR scanner (Philips 3.0 Tesla MRI System) and preliminary MRIs of the cadaver's pelvis were scanned. Because of the prone position, two anterior superior iliac spines and one pubic symphysis were in a coronal MRI without difficulty. We adjusted the cadaver's direction until bilateral structures, such as the femur heads, were symmetric in axial and coronal MRIs. The cadaver's direction was recorded by drawing horizontal and vertical lines on the skin of the cadaver's sacral region along the laser indicator of the MR machine (Fig. 1A).

The pelvis of the cadaver was MR-scanned. The pelvis was covered with the pelvic coil of a 3 Tesla MR machine. After setting the MR scanning parameters (intervals, 1 mm; field of view, width 500 mm × height 500 mm × length 230 mm; resolution, 512 × 512; pixel size, 1 mm; bit depth, 8 bits gray), T1-weighted MRIs were obtained (repetition time, 800 msec; echo time, 20 msec), and subsequently T2-weighted MRIs were achieved (repetition time, 37,344 msec; echo time, 100 msec). The entire MRIs were saved as tag image file format (TIFF) (Fig. 2A, B, Table 1).

The cadaver pelvis was then CT-scanned. The cadaver was moved to the CT scanner (Philips Brilliance 64 channel). The direction of the pelvis was adjusted until the horizontal and vertical lines on the sacral skin corresponded to the laser lights of the CT machine (Fig. 1A). After setting the scanning parameters (thickness, 1 mm; intervals, 0 mm; field of view, width 500 mm × height 500 mm × length 230 mm; resolution, 512 × 512; pixel size, 1 mm;

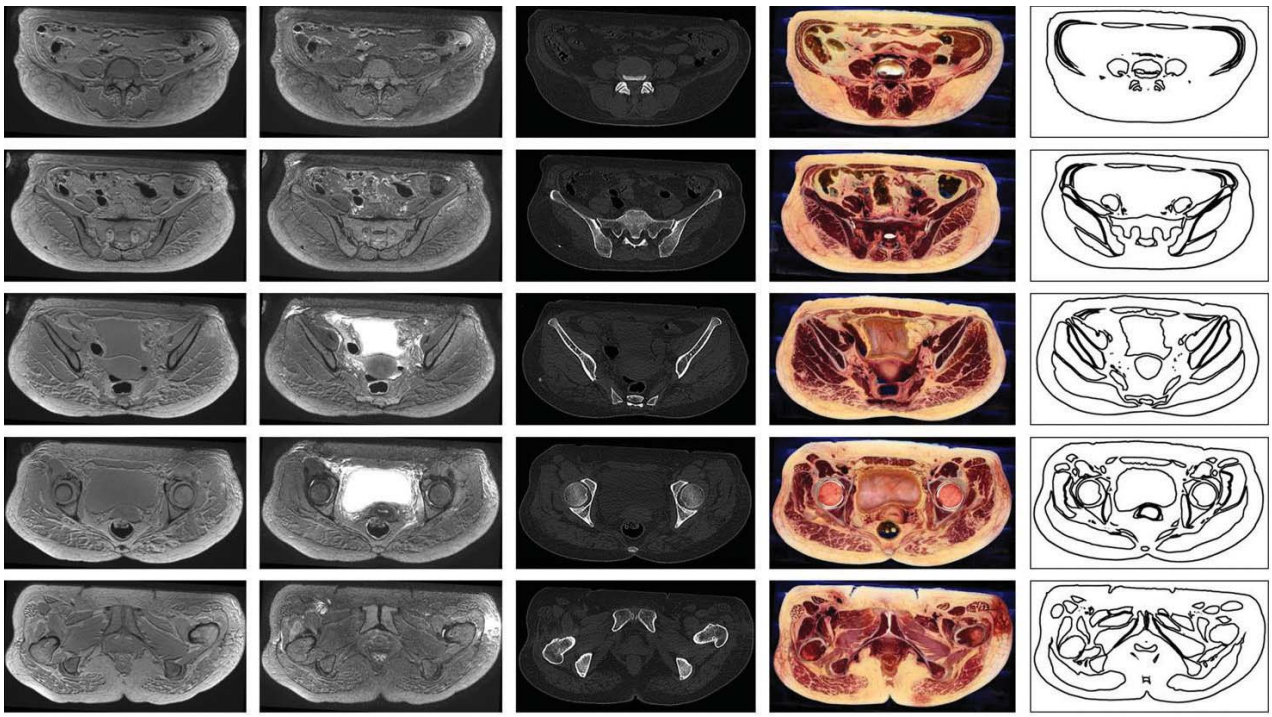

Fig. 2. (A) T1 MRIs, (B) T2 MRIs, (C) CTs, (D) sectioned images, and (E) outlined images of female cadaver pelvis.

Table 1. Features of the MRIs, CTs, sectioned images (SIs), and outlined images

Images	Intervals	Number	Resolution	Pixel size	Bit depth	One file size
T1 MRIs*	1.0 mm	222	512 × 512	1.0 mm	8 bit gray	256 KBytes
T2 MRIs*	1.0 mm	222	512 × 512	1.0 mm	8 bit gray	256 KBytes
CTs*	1.0 mm	222	512 × 512	1.0 mm	8 bit gray	256 KBytes
SIs*	0.1 mm	2,220	4,368 × 2,912	0.1 mm	48 bit color	73 MBytes
Coronal SIs	0.1 mm	2,912	4,368 × 2,220	0.1 mm	48 bit color	73 MBytes
Sagittal SIs	0.1 mm	4,368	2,220 × 2,912	0.1 mm	48 bit color	37 MBytes
Outlined images*	1.0 mm	222	4,368 × 2,912	0.1 mm	24 bit color	45 MBytes

*Direction of the images is horizontal. All images are TIFF files except the outlined images (PSD files).

120 kV; 30 mAs), the pelvis was CT-scanned to be saved as TIFF files (Fig. 2C, Table 1). Just after scanning, the cadaver that was still in the prone position was placed into a deep freezer at −70 degrees Celsius.

In the MRIs and CTs, we did not identify pathologic findings. The only exception was a cyst in the upper part of the left ovary, which was discovered in T2-weighted MRIs. We regarded this cadaver as an appropriate subject and decided to proceed with serial sectioning.

The abdomen and pelvis blocks were separated from the cadaver for preliminary and main experiments, in that order. After removing the totally frozen cadaver from the freezer, the pelvis block from the third lumbar vertebra to the upper body of the femur was extracted with a saw. The pelvis block included a lower part of the abdomen, pelvis, perineum, gluteal regions, and upper part of the bilateral thighs. In addition, the abdomen block (thickness, 10 mm) was separated just above the pelvis block. The two blocks were refrozen.

The pelvis and abdomen blocks were embedded. A large embedding box comprising the frontal, rear, and two side boards was prepared. In the box, the pelvis block in the prone position was placed for grinding the cadaver in the superoinferior direction. A thread from the front to rear

boards was tied parallel to the long axis of the embedding box; another thread between the two side boards was tied parallel to the short axis. After lighting an incandescent lamp on the threads, the direction of the pelvis block was adjusted until the shadow of the threads corresponded to the horizontal and vertical lines drawn on the block. The abdomen block was placed on the top of the pelvis block in the anatomical position, and the location of the abdomen block was adjusted just above the pelvis block. Subsequently, an embedding agent (water, 1,000 L; gelatin, 30 kg; methylene blue, 0.5 kg) was poured around the blocks until the embedding box was filled with the embedding agent and frozen in the freezer to fix them rigidly (Fig. 1B).

As a preliminary trial, the abdomen block was serially sectioned to determine the optimal conditions of sectioning in the cryomacrotome (Park et al. 2005b). For acquiring high-quality sectioned surfaces with 0.1 mm-sized intervals, we optimized the rotating speed of the grinding disc, the moving speed of the embedding box, and the blade changing cycles in the grinding disc (Fig. 1C).

The sectioned surfaces of the abdomen block were photographed to determine the optimal photographic conditions. The suitable strobes (Elinchrom^{TM} Digital S) and power supply (Elinchrom^{TM} Digital 2) were installed to maintain constant brightness of the sectioned surfaces. The strobes and the digital camera lens (Canon EF 50 mm f/1.2 L USM) were covered with polarizing filters to reduce scattered reflected lights. A 437×291 mm^2-sized sectioned surface was photographed using the Canon EOS 5D digital camera with $4,368 \times 2,912$ resolution (Fig. 1C) so that the SIs with 0.1×0.1 mm^2-sized pixels were created. In a preliminary experiment, we found out the photographic conditions of the digital camera (ISO, 100; shutter speed, 1/125; aperture opening, 8.0; focus, manual).

The main experiment was conducted as follows. The pelvis block was milled at 0.1 mm intervals. After wiping away the frost on every sectioned surface, the color patch and gray scale were placed around the sectioned surface, all of which were photographed to create one SI (Fig. 1C). It took 50 days in the winter to acquire 2,220 SIs of the cadaver pelvis. On the Adobe Photoshop CS3 extended version 10 (Photoshop), the SIs were rotated at 180 degrees and then converted right-to-left to conform with radiologic convention. The SIs were saved as TIFF files (intervals, 0.1 mm; pixel size, 0.1 mm; bit depth, 48 bit color; Fig. 2D, Table 1).

Using self-developed software, a row of every axial SIs of the pelvis was stacked to produce a coronal SI. Using a

(A)

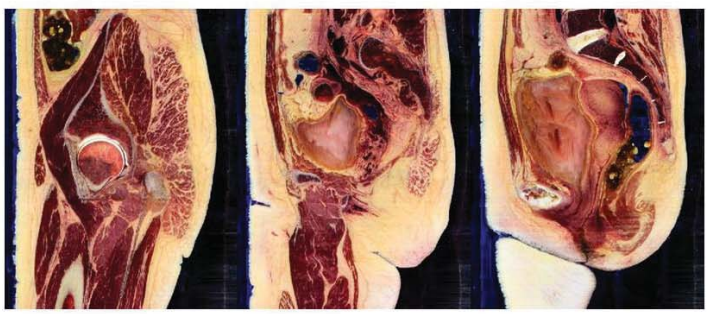

(B)

Fig. 3. (A) Coronal and (B) sagittal planes of the sectioned images of the female pelvis, created from the axial sections.

similar method, the columns of all axial SIs were stacked to produce sagittal SIs (Fig. 3, Table 1).

By referring to the coronal and sagittal planes, alignment and brightness of SIs were checked out. In spite of the careful use of the cryomacrotome and digital camera, SIs occasionally showed incorrect alignments. The misaligned SIs, easily found in coronal and sagittal planes (Fig. 3), were corrected by using the "move" tool of Photoshop. Even if high grade strobes and a power-pack were used under supervision of a photography professional, the brightness of neighboring SIs was often inconstant. The incorrectly bright and dark SIs could not be missed in coronal and sagittal planes (Fig. 3) to be amended by using the "curves" tool of Photoshop.

In the coronal and sagittal SIs, the horizontal bands were diminished. Although the inconstant brightness of the SIs was revised, the coronal and sagittal SIs showed horizontal bands inevitably due to slightly different brightness, which could not be detected by the naked eye. The horizontal bands might cause problems because the coronal and sagittal SIs themselves were to be distributed as the raw data (Table 1). Therefore, these horizontal bands were decreased effectively using a "Fourier transform" command on Photoshop (Fig. 4) (Cho and Har 2007).

We decided to outline structures of interest, which were prominent in the SIs. The 73 structures from the lower

(A) (B)

Fig. 4. (A) Coronal sectioned images showing horizontal bands, (B) which are diminished by a Fourier spectrum algorithm.

Table 2. Seventy-three structures, outlined on the sectioned images

System	Structures
Integumentary	Skin
Skeletal	Lumbar vertebrae (L4-L5), Sacrum, Coccyx, Hip bone*, Femur*
Articular	Intervertebral disc (L5-Sacrum), Pubic symphysis
Muscular	Rectus abdominis*, External oblique abdominal muscle*, Internal oblique abdominal muscle*, Transversus abdominis*, Levator ani*, Coccygeus*, External anal sphincter*, Iliacus*, Psoas major*, Gluteus maximus*, Gluteus medius* Gluteus minimus*, Tensor fasciae latae*, Piriformis*, Obturator internus*, Superior gemellus*, Inferior gemellus*, Quadratus femoris*, Sartorius*, Rectus femoris*, Vastus lateralis*, Vastus intermedius*, Vastus medialis*, Pectineus*, Adductor longus*, Adductor brevis*, Adductor magnus*, Gracilis*, Obturator externus*, Biceps femoris*, Semitendinosus*, Semimembranosus*
Alimentary	Ascending colon, Transverse colon, Descending colon, Sigmoid colon, Rectum, Anal canal, Anus
Vascular	Common iliac artery*, Internal iliac artery*, Obturator artery*, Superior gluteal artery (left), Inferior gluteal artery (left), Superior vesical artery*, Inferior vesical artery (left), Middle rectal artery*, Internal pudendal artery*, External iliac artery (left), Femoral artery (right), Deep femoral artery*, Common iliac vein (left), Internal iliac vein (right), External iliac vein*, Great saphenous vein*, Femoral vein*
Urogenital	Ureter*, Urinary bladder, Ovary*, Uterus (fundus, body, cervix), Vagina, Urethra
Nervous	Lumbar nerves (L4-L5)*, Sacral nerves (S1-S4)*

*Bilateral structures

abdomen to the upper thigh included not only female urogenital structures, but also neighboring structures such as bones, muscles, arteries, and veins. We determined to segment bilateral structures on both the right and left sides (Table 2).

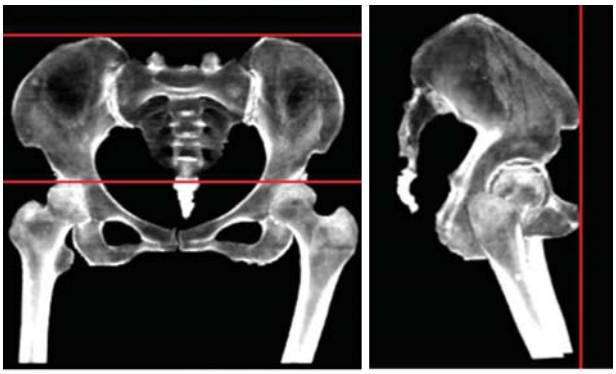

(A) (B)

Fig. 5. Volume model of bones showing that (A) bilateral iliac crests or femur heads are in the same horizontal plane and (B) anterior superior iliac spine and pubic symphysis are in a coronal plane.

The structures were outlined using the procedures we developed on Photoshop in the previous study (Park et al. 2005a). On SIs, prominent structures, like skin, were outlined automatically using the "magic wand" tool in Photoshop. When automatic outlining was not possible, semi-automatic outlining was performed using the "magnetic lasso" or "quick selection" tool (e.g., bones). Most structures had to be outlined manually by the "lasso" tool. As a result, 220 outlined images (Photoshop document (PSD) files) were acquired (Fig. 2E, Table 1).

Segmentation was verified on coronal and sagittal planes. On Photoshop, outlines in outlined images were colored, and then the colored outlines with the underlying SIs were stacked to acquire coronal and sagittal planes using self-developed software. The coronal and sagittal planes were observed to find outlining errors, which were promptly repaired.

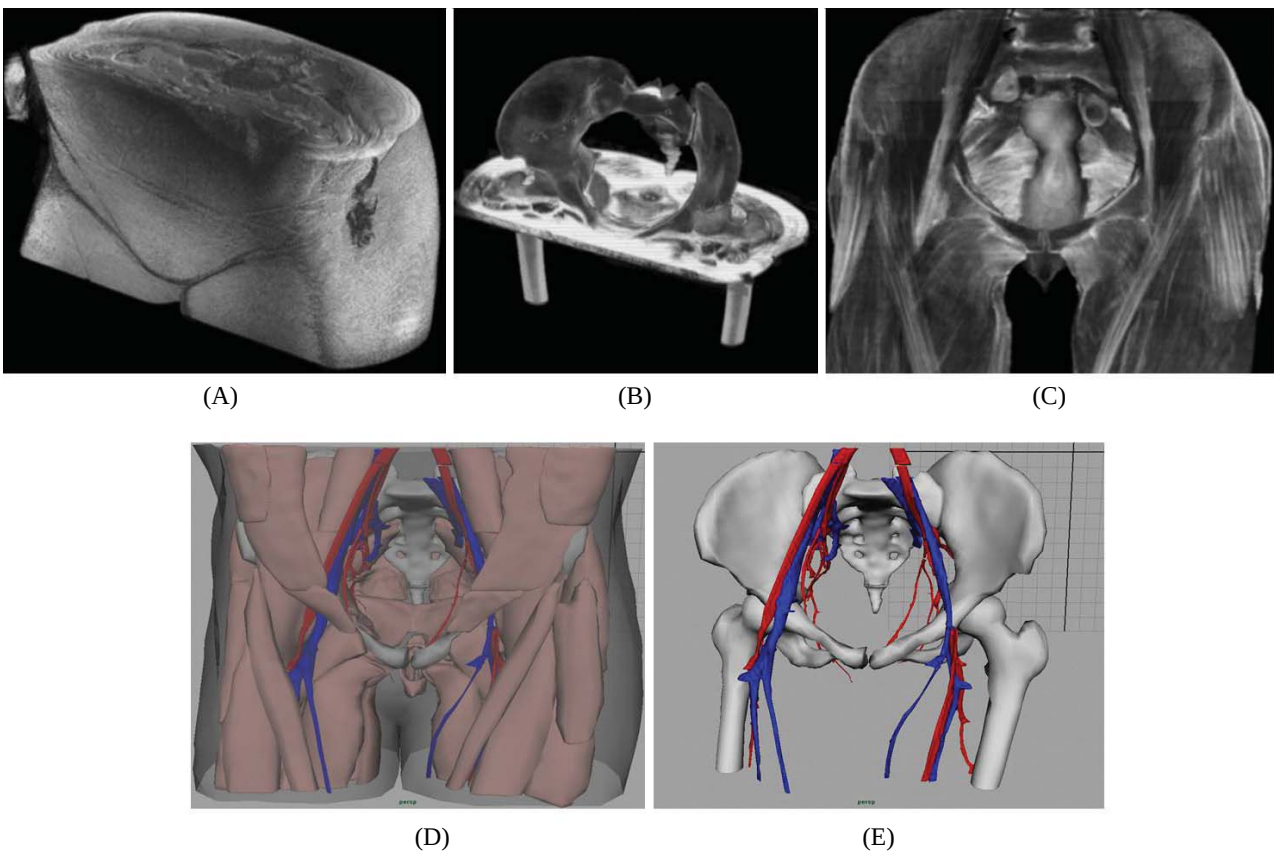

(A) (B) (C)

(D) (E)

Fig. 6. (A) Volume model of the female pelvis, including skin; (B) volume model of bones, superimposed on a horizontal sectioned image; (C) volume model of muscles and genital organs; (D) Surface model of female pelvis, including skin and muscles; (E) surface models bones and blood vessels.

As a preliminary step before volume reconstruction, the intervals of SIs were changed from 0.1 to 1 mm, the pixel size was changed from $0.1 \times 0.1\,mm^2$ to $1 \times 1\,mm^2$, and the bit depth was changed from 48 bit color to 8 bit gray. Using the outlined images, the outside of the skin in SIs was automatically erased using Photoshop. On MRIcro software version 1.4 (MRIcro), the SIs were stacked and reconstructed by volume modeling to acquire a 3D volume model of the pelvis with $1 \times 1 \times 1\,mm^3$ voxel size in 8 bit gray. Likewise, after the outside of the selected internal structures was erased, the volume model of the structures was made. In particular, the volume model was arbitrarily sectioned to display sectional planes or superimposed on the sectioned image (Figs. 5, 6A-C) (Park et al. 2009).

The outlined images independent of the SIs were used for production of surface models on Autodesk Maya version 2009 (Maya) and other software. From the outlined images, outlines of a selected structure were stacked. Sub-

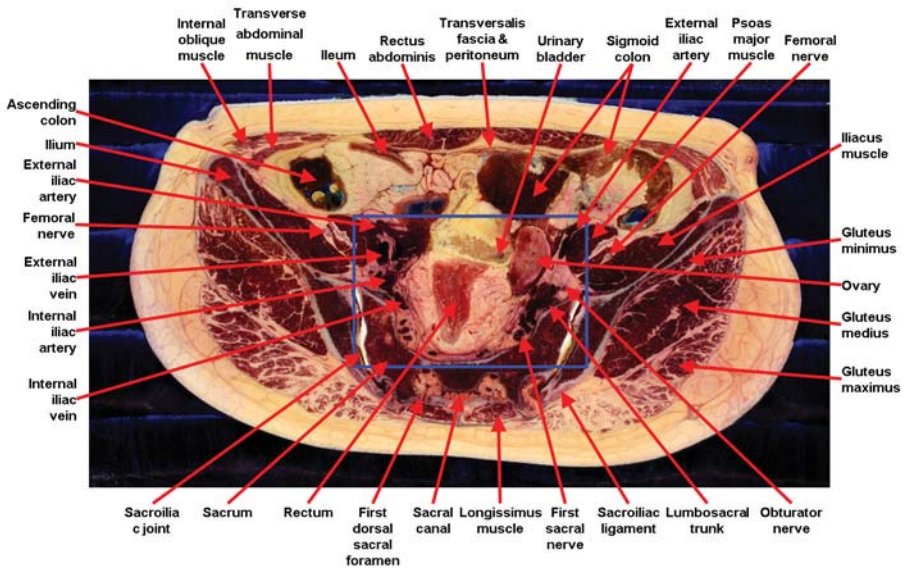

(A)

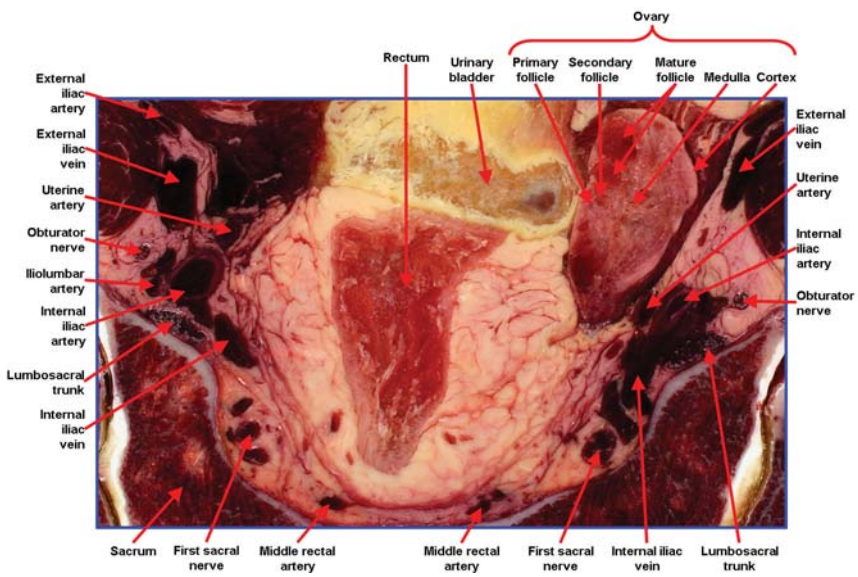

(B)

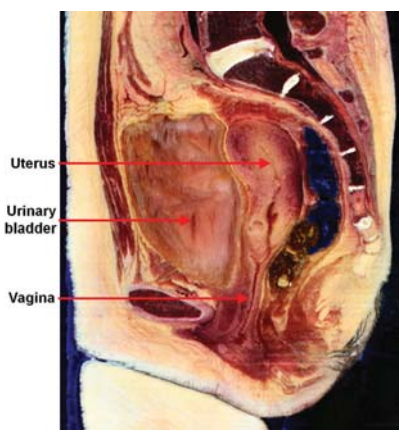

(C)

Fig. 7. (A) Labeled structures in the sectioned image and (B) labeled structures around the rectum, urinary bladder, and ovary in the zoomed image. (C) Variation of uterus (retroversion and anteflexion) in the midsagittal plane.

sequently, gaps between the outlines were filled with polygons (surface reconstruction) to produce 3D surface model of the structure (Park et al. 2007, Shin et al. 2009a, b). In the same manner, the surface models of other outlined structures are being built by authors (Fig. 6D, E).

Results

The female cadaver was a suitable subject for acquiring SIs of the pelvis. T2-weighted MRIs and SIs showed a cyst in the left ovary, but there were no other specific pathologic findings. We did not find any remarkable anatomic variations. The patient's age (43 years) prior to menopause enabled SIs to involve dynamic female reproductive structures, such as primary, secondary, and mature follicles in both ovaries (Fig. 7B). The revived natural contour of cadaver's buttocks appeared in SIs (Figs. 2, 8D).

A total of 2,220 SIs of the female pelvis were obtained without any technical difficulty. The pelvis and adjacent region of the female cadaver were sectioned by grinding instead of being sliced to obtain SIs at intervals of 0.1 mm (Fig. 2D, Table 1).

Good quality SIs were obtained after preliminary optimizations by using an advanced digital camera that allowed a $0.1 \times 0.1\,mm^2$ pixel size in 48 bits of color. Stereoscopically, SIs showed structures as small as 0.1 mm for the $0.1 \times 0.1 \times 0.1\,mm^3$-sized voxels (Figs. 2D, 7, Table 1).

Furthermore, small-sized intervals and pixels enabled us to prepare sagittal and coronal SIs of high quality (Fig. 3, Table 1), which showed no difference in detail with the original axial SIs. Horizontal bands in the coronal and sagittal SIs were diminished to raise the value of the vertical images as the distributed data (Fig. 4). The final SIs maintained correct alignment and constant brightness that could be verified by the coronal and sagittal SIs.

We confirmed the horizontal direction of the SIs. In the horizontal and coronal SIs, the bilateral structures were nearly symmetric (Figs. 2D, 3A). In the volume model of bones, the bilateral iliac crests and femur heads were located in the same horizontal planes. The anterior superior iliac spine and pubic symphysis were in a coronal plane (Fig. 5A). The horizontal direction of SIs was possible because horizontal and vertical lines were drawn on the cada-

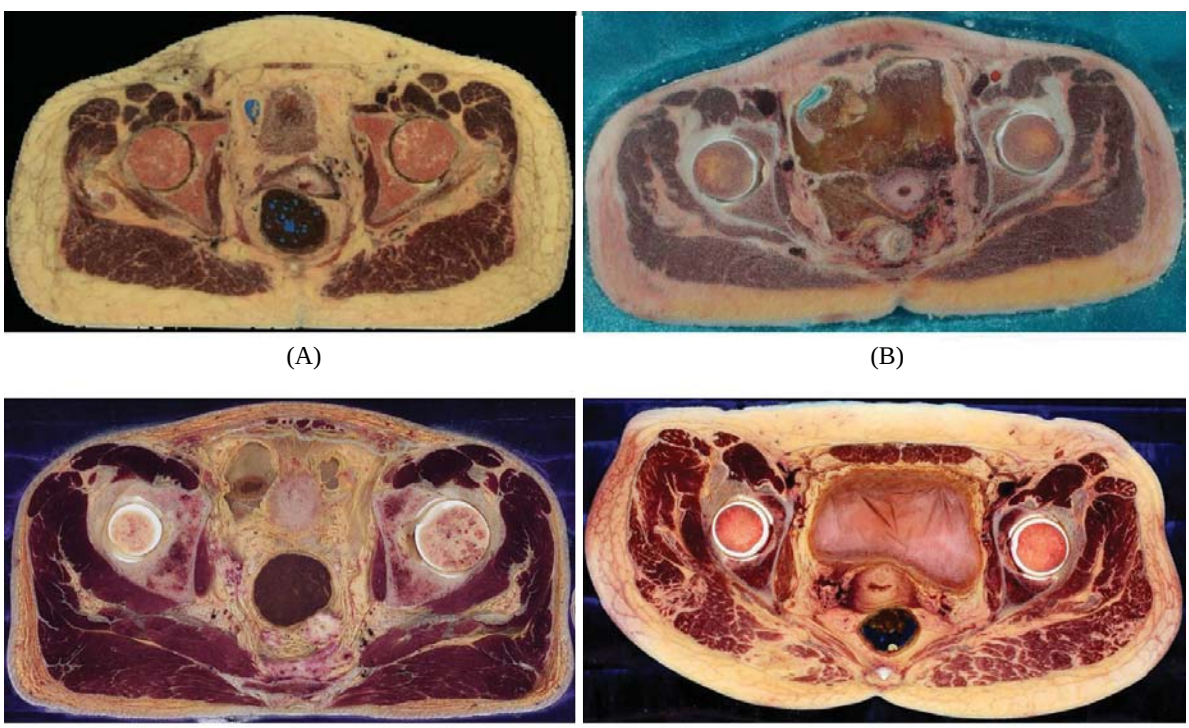

Fig. 8. Sectioned images of female pelvis in (A) Visible Human Project, (B) Chinese Visible Human, (C) Visible Korean male, and (D) this study, namely the Visible Korean female.

ver skin using MRIs and the direction of the pelvis block was adjusted using the lines before sectioning (Fig. 1A, B).

The SIs are accompanied by 3 Tesla MRIs and CTs at 1 mm intervals (Table 1). In T1-weighted MRIs, muscle and intestinal wall were well visualized (Fig. 2A). In T2-weighted MRIs, fine soft tissues (e.g. ovarian follicles) were identifiable with 3 Tesla (Fig. 2B). In CTs, bones were easy to demarcate as expected (Fig. 2C).

Two hundred twenty-two outlined images of 73 structures were prepared at 1 mm intervals (Fig. 2E, Tables 1, 2). The outlined images were satisfactory in quality, which was verified by the coronal and sagittal planes of the outlined images.

Once the structures were outlined, 3D volume and surface models of the structures could be produced. Without the help of the computer programmers, volume and surface reconstruction was performed successfully using MRIcro and Maya together with other supplementary software, respectively. The volume and surface models could be rotated at arbitrary angles to recognize the stereoscopic shape and location relationship of the structures. The volume models could be sectioned on MRIcro to display sectional planes (Figs. 5, 6A-C) whereas the surface models could be manipulated in real time on Maya (Fig. 6D, E).

Discussion

The SIs of the female pelvis would serve as the source of virtual dissection software for medical students and virtual surgery simulators for gynecologists or urologists. For more useful applications, the SIs are required to retain the following conditions.

First, the SIs are required to be horizontal. Even though the patients' MRIs and CTs are not precisely horizontal in clinics, the cadaver's SIs need to be rigorously horizontal as the reference source. If the SIs were not horizontal, 3D images made of the SIs would not assume the anatomical position, which is the basic human posture in anatomy. Moreover without horizontal direction, authors would have lost the most important criterion to maintain the correspondence of the SIs, MRIs, and CTs (Fig. 2A-D). In the other studies of SIs, the horizontal plane had not been fully emphasized. But in this study, the methods and results to acquire horizontal SIs, MRIs, and CTs were satisfactory and described in detail. The prone position of the cadaver was favorable for the acquisition of the horizontal images of the pelvis (Figs. 1, 5).

Second, the SIs are required to show good body contour. In the previous research, the cadavers were placed in the supine position around death, and the supine position was maintained even during serial sectioning. Consequently, the buttocks were pressed in the SIs, thus presenting an unnatural appearance of not only skin, but also the underlying gluteus maximus (Fig. 8A-C) (Spitzer and Whitlock 1998, Park et al. 2005a, Zhang et al. 2006, Yuan et al. 2008). Consequently, 3D images of the buttocks skin and gluteus maximus would be awkward. In the present study, the problem was simply solved by the prone position of the cadaver; the solution was enabled by a small pelvis rather than the whole body (Fig. 1). In addition, the original body contour of the cadaver matters. It is known that the female cadaver in Visible Human Project was too obese, while the female cadaver in the present study was not overweight (height, 1.52 m; weight, 54 kg). The outstanding SIs and 3D images of the standard woman with a natural gluteal contour are anticipated to be appreciated by users.

Third, the SIs are required to visualize normal structures. The SIs and their volume models are likely to be representative of normal female pelves. Therefore, it is desirable that the SIs are free from pathology. Fortunately, in this study, a cyst in the left ovary was the only pathologic finding. Other pelvic structures were not affected by alcoholism. There was a few variation of the cadaver pelvis that the uterus was retroverted and anteflexed (Fig. 7C). Even though, urogenital organs of female are core structures, the uterus and ovaries of the Visible Human Project female were degenerated due to old age (59 years old) (Fig. 8A). But our research involved a female cadaver earlier than menopause (43 years old), so normal follicles in the ovary were found (Fig. 7B). Accordingly, the SIs are expected to be used for establishing valuable virtual simulation; for example, simulator for laparoscopic aspiration of the mature ovarian follicles.

Fourth, the SIs are required to demonstrate real colors of living humans. Normal body colors would help users identify the structures, such as peripheral nerves in SIs (Fig. 7). Volume models retaining the normal colors in their surfaces and their sectional planes would be the source of realistic simulation. In the Visible Human Project, the

colors of the SIs were relatively white because formalin was perfused into the cadaver (Fig. 8A) (Spitzer and Whitlock 1998). In the Chinese Visible Human and Virtual Chinese Human, red gelatin solution was perfused to demonstrate the arterial network of the SIs. As a side effect, the red gelatin solution leaked from the arteries to tissues, especially to muscles, which turned red in the SIs (Fig. 7B) (Zhang et al. 2006, Yuan et al. 2008). In the present study, for acquiring the real colors, nothing was injected and we then prepared the best equipments and the experienced techniques for serial sectioning, lighting, and photographing during the preliminary trial.

Fifth, the SIs are required to display small structures. After stacking the SIs, a 3D volume model composed of voxels could be reconstructed. In the previous studies, the voxel size was $0.33 \times 0.33 \times 0.33\ mm^3$ (Spitzer and Scherzinger 2006) or $0.2 \times 0.2 \times 0.2\ mm^3$ (Park et al. 2005b), whereas in this paper, the voxel size was $0.1 \times 0.1 \times 0.1\ mm^3$. Based on our experience, a voxel size $< 0.1 \times 0.1 \times 0.1\ mm^3$ seems to enter the microscopic level and has limited importance with respect to gross anatomy. In addition, the SIs was 48 bit color, which is better than the 24 bit color in the earlier research (Spitzer and Whitlock 1998, Park et al. 2005b). Because of the $0.1 \times 0.1\ mm^2$-sized pixels in 48 bit color herein, many small structures were exactly identified in SIs (Figs. 2D, 7), and subsequently 73 structures were outlined (Table 2). Based on our outlined images and original SIs, other investigators are able to outline more structures for their own needs. Otherwise, they may divide the outlined structures into substructures to obtain more detailed segmented images, i.e., the uterine tube into the infundibulum, ampulla, isthmus, intramural part and the uterus into the endometrium, myometrium, and perimetrium.

Sixth, the SIs are required to be accompanied by MRIs, CTs, coronal SIs, and sagittal SIs (Table 1). The MRIs and CTs of the same cadaver corresponding to the SIs (Fig. 2A-D) could be used for another educational program. Specifically, on the program, normal structures in 3 Tesla MRIs (T1- and T2-weighted) and CTs could be learned by comparison with SIs of the same subject (Park et al. 2008). Additionally, coronal and sagittal SIs with the horizontal bands diminished (Fig. 4) are needed for two-dimensional atlas to interpret vertical MRIs and CTs.

Seventh, the SIs are required to be accompanied by outlined images and surface models. Outlined images could be made of the SIs by any researchers (Fig. 2E). The problem is that outlining, which can be performed only by medical experts, is very time-consuming (Park et al. 2005a). Thus, in order to reduce the repetitive works of different researchers, we are willing to distribute even outlined images. All data of the Visible Korean including images of this study are available free of charge after obtaining permission from our group. For the same reason, we have the plan to distribute the 3D surface models, which are currently being built (Fig. 6B). In contrast, 3D volume models will not be distributed because genuine volume models containing high resolution and real colors have a huge file size. Another reason is that the volume models can be readily generated from the distributed SIs and outlined images by others.

The SIs of female pelvis and corresponding MRIs, CTs, and outlined images produced during this study will hopefully stimulate researchers to develop 3D medical simulation tools for improvement of clinical practice in obstetrics, gynecology, and urology.

Acknowledgement

This research was supported by Basic Science Research Program through the National Research Foundation of Korea (NRF) funded by the Ministry of Education, Science and Technology (grant number 2010-0009950). In addition, authors would like to express the deep appreciation to Seung-ho Han (M.D., Ph.D.) of the Catholic Institute for Applied Anatomy in Catholic University of Korea for his contribution to the donated female cadaver.

References

Ackerman MJ : The Visible Human Project: A resource for education. Acad Med 74: 667-670, 1999.

Cho DH, Har DH : A study on the enhancement of sliced human anatomy imagery by removal of high-frequency component. AURA 17: 102-110, 2007. (in Korean)

Heinrichs WL, Pothen A, Mather R, Constantinou P, Lewis M, Chase RA, Dev P : 3D female pelvic organ models: Comparison of the Visible Human female with a reproductive age pelvis. The Visible Human Project Conference Proceedings, 1996.

Park JS, Chung MS, Hwang SB, Lee YS, Har DH : Technical

report on semiautomatic segmentation using the Adobe Photoshop. J Digit Imaging 18: 333-343, 2005a.

Park JS, Chung MS, Hwang SB, Lee YS, Har DH, Park HS : Visible Korean Human: Improved serially SIs of the entire body. IEEE Trans Med Imaging 24: 352-360, 2005b.

Park JS, Chung MS, Hwang SB, Shin BS, Park HS : Visible Korean Human: Its techniques and applications. Clin Anat 19: 216-224, 2006.

Park JS, Chung MS, Shin DS, Har DH, Cho ZH, Kim YB, Han JY, Chi JG : Sectioned images of the cadaver head including the brain and correspondences with ultra-high field 7.0 Tesla MRIs. Proc IEEE 97: 1988-1996, 2009.

Park JS, Jung YW, Lee JW, Shin DS, Chung MS, Riemer M, Handels H : Generating useful images for medical applications from the Visible Korean Human. Comput Methods Programs Biomed 92: 257-266, 2008.

Park JS, Shin DS, Chung MS, Hwang SB, Chung J : Technique of semiautomatic surface reconstruction of the Visible Korean Human data using commercial software. Clin Anat 20: 871-879, 2007.

Pommert A, Höhne KH, Burmester E, Gehrmann S, Leuwer R, Petersik A, Pflesser B, Tiede U : Computer-based anatomy: A prerequisite for computer-assisted radiology and surgery. Acad Radiol 13: 104-112, 2006.

Schiemann T, Freudenberg J, Pflesser B, Pommert A, Priesmeyer K, Riemer M, Schubert R, Tiede U, Höhne KH : Exploring the Visible Human using the VOXEL-MAN framework. Comput Med Imaging Graph 24: 127-132, 2000.

Shin DS, Chung MS, Lee JW, Park JS, Chung J, Lee SB, Lee SH : Advanced surface reconstruction technique to build detailed surface models of liver and neighboring structures from the Visible Korean Human. J Korean Med Sci 24: 375-383, 2009a.

Shin DS, Chung MS, Park JS, Lee SB, Lee SH, Chung J : Surface model of the gastro-intestinal tract constructed from the Visible Korean. Clin Anat 22: 601-609, 2009b.

Spitzer VM, Scherzinger AL : Virtual anatomy: An anatomist's playground. Clin Anat 19: 192-203, 2006.

Spitzer VM, Whitlock DG : Atlas of the Visible Human Male: Reverse Engineering of the Human Body. Massachusetts, Jones and Bartlett Publishers, 1998.

Uhl JF, Park JS, Chung MS, Delmas V : Three-dimensional reconstruction of urogenital tract from Visible Korean Human. Anat Rec Part A 288A: 893-899, 2006.

Yuan Y, Lina Q, Shuqian L : The reconstruction and application of Virtual Chinese Human female. Comput Methods Programs Biomed 92: 249-256, 2008.

Zhang SX, Heng PA, Liu ZJ : Chinese Visible Human Project. Clin Anat 19: 204-215, 2006.

여성 비뇨생식기관과 그 주변 구조물을 낱낱이 볼 수 있는 여성 골반의 절단면영상

황성배, 정민석[1], 황윤익[1], 박효석[2], 하동환[3], 신동선[1], 신병석[4], 박진서[2]

경북전문대학 물리치료과, [1]아주대학교 의과대학 해부학교실, [2]동국대학교 의과대학 해부학교실
[3]중앙대학교 첨단영상대학원 디지털과학사진연구실, [4]인하대학교 컴퓨터정보공학부

간추림 : 여성 골반의 절단면영상은 여성 비뇨생식계통의 실감나는 3차원영상을 만들 수 있는 가장 좋은 재료이다. 이 연구의 목적은 여성 골반의 고화질 절단면영상과 테두리영상을 마련해서 여성 비뇨생식계통의 가상해부, 가상수술을 위한 3차원영상을 만드는 데 도움 주는 것이다.

한국 여성 시신의 골반을 대상으로 자기공명영상과 컴퓨터단층사진을 찍었다. 이 골반을 포매한 다음에 수평방향으로 연속절단하였고(간격 0.1 mm), 각각의 절단면을 사진 찍어서 절단면영상을 만들었다. 절단면영상에서 보이는 73개 구조물(비뇨생식기관과 주변 구조물)의 테두리를 그려서 테두리영상을 만들었다. 절단면영상과 테두리영상으로 각 구조물의 3차원부피영상, 3차원표면영상을 만들었다.

여성 골반의 자기공명영상 222개(간격 1 mm), 컴퓨터단층사진 222개(간격 1 mm), 절단면영상 2,220개(화적소 크기 $0.1 \times 0.1 \times 0.1\ mm^3$, 빛깔 개수 48 bits color), 그리고 테두리영상 222개(간격 1 mm)를 만들었으며, 이 영상은 서로 들어맞았다. 절단면영상과 테두리영상으로 만든 3차원영상은 실감나는 가상현실 프로그램을 만드는 데 도움 될 것이고, 나아가 여성 골반의 해부학과 임상을 익히는 데 이바지할 것이다.

찾아보기 낱말 : 절단해부학, 자기공명영상, 컴퓨터단층사진, 3차원영상, 골반, 비뇨생식계통

교신저자 : 박진서(동국대학교 의과대학 해부학교실)
전자우편 : park93@dongguk.ac.kr